Defense Activated by 9-Lipoxygenase-Derived Oxylipins Requires Specific Mitochondrial Proteins[1][W]

Tamara Vellosillo[2], Verónica Aguilera, Ruth Marcos, Michael Bartsch[3], Jorge Vicente, Tomas Cascón, Mats Hamberg, and Carmen Castresana*

Centro Nacional de Biotecnología-Consejo Superior de Investigaciones Científicas, Campus Universidad Autónoma, Cantoblanco, E–28049 Madrid, Spain (T.V., V.A., R.M., M.B., J.V., T.C., C.C.); and Division of Physiological Chemistry II, Department of Medical Biochemistry and Biophysics, Karolinska Institutet, S–171 77 Stockholm, Sweden (M.H.)

9-Lipoxygenases (9-LOXs) initiate fatty acid oxygenation, resulting in the formation of oxylipins activating plant defense against hemibiotrophic pathogenic bacteria. Previous studies using *nonresponding to oxylipins* (*noxy*), a series of Arabidopsis (*Arabidopsis thaliana*) mutants insensitive to the 9-LOX product 9-hydroxy-10,12,15-octadecatrienoic acid (9-HOT), have demonstrated the importance of cell wall modifications as a component of 9-LOX-induced defense. Here, we show that a majority (71%) of 41 studied *noxy* mutants have an added insensitivity to isoxaben, an herbicide inhibiting cellulose synthesis and altering the cell wall. The specific mutants *noxy2*, *noxy15*, and *noxy38*, insensitive to both 9-HOT and isoxaben, displayed enhanced susceptibility to *Pseudomonas syringae* DC3000 as well as reduced activation of salicylic acid-responding genes. Map-based cloning identified the mutation in *noxy2* as *At5g11630* encoding an uncharacterized mitochondrial protein, designated NOXY2. Moreover, *noxy15* and *noxy38* were mapped at the *DYNAMIN RELATED PROTEIN3A* and *FRIENDLY MITOCHONDRIA* loci, respectively. Fluorescence microscopy and molecular analyses revealed that the three *noxy* mutants characterized exhibit mitochondrial dysfunction and that 9-HOT added to wild-type Arabidopsis causes mitochondrial aggregation and loss of mitochondrial membrane potential. The results suggest that the defensive responses and cell wall modifications caused by 9-HOT are under mitochondrial retrograde control and that mitochondria play a fundamental role in innate immunity signaling.

Plants have evolved distinct mechanisms to sense the presence of potential pathogens and respond by activating innate immunity. Compounds recognized by specific plant receptors include nonself structures derived from attacking pathogens, such as conserved microbial molecules (designated as microbe-associated molecular patterns) and specific effector molecules delivered into the plant cell (Boller and Felix, 2009). Additionally, plants recognize self-structure signals released from pathogen-damaged tissues or induced during infection to potentiate defense and limit pathogen damage (designated as damage-associated molecular patterns; Brutus et al., 2010; Yamaguchi et al., 2010). The plant responses to distinct recognized molecules share considerable overlap and converge in transcriptome reprogramming and generation of defense compounds (Dodds and Rathjen, 2010). Critical signals orchestrating the plant responses to pathogen attack are defense hormones such as salicylic acid (SA), jasmonates (JAs), and ethylene (ET; Glazebrook, 2005) and their cross talk with other signaling pathways (López et al., 2008; Robert-Seilaniantz et al., 2011). Moreover, other signaling molecules, including reactive oxygen species (ROS) and nitric oxide, participate in triggering and regulating plant immunity (Torres et al., 2006; Vellosillo et al., 2010; Spoel and Loake, 2011). The interplay between distinct signaling molecules and their respective downstream networks is complex and not fully understood.

The defense hormone JA belongs to a large family of active lipid derivatives, collectively known as oxylipins, whose importance in controlling pathological processes in plants is gradually being recognized (López et al., 2008; Andreou et al., 2009). Oxylipins are produced by initial oxidation of fatty acids, mainly linolenic and linoleic acids, by the action of lipoxygenases (9-lipoxygenase [9-LOX] and 13- lipoxygenase), α-dioxygenases, or monooxygenases followed by secondary modifications catalyzed mainly by cytochrome P450 enzymes or peroxygenase (Blée, 2002; Hamberg et al., 2002; Andreou et al., 2009). In addition, production of oxylipins from polyunsaturated fatty acids can take place nonenzymatically in the presence of singlet oxygen or by free radical-mediated oxygenation (Durand et al., 2009).

The JA pathway of the oxylipin metabolome is initiated by 13-lipoxygenase and results in the formation

[1] This work was supported by grant nos. BIO2009–09670 and CSD2007–00057. M.B. was supported by a Marie Cure Fellowship of the European Union (grant no. PIEF–GA–2008–221448).

[2] Present address: Energy Biosciences Institute, University of California, Berkeley, CA 94720.

[3] Present address: Syngenta, CH–4332 Stein, Switzerland.

* Corresponding author; e-mail ccastresana@cnb.csic.es.

The author responsible for distribution of materials integral to the findings presented in this article in accordance with the policy described in the Instructions for Authors (www.plantphysiol.org) is: Carmen Castresana (ccastresana@cnb.csic.es).

[W] The online version of this article contains Web-only data.
www.plantphysiol.org/cgi/doi/10.1104/pp.112.207514

of (+)-7-iso-JA and its Ile conjugate, compounds that control the resistance of plants to necrotrophic pathogens and insect attack (for review, see Browse, 2009; Fonseca et al., 2009; Wu and Baldwin, 2010). In addition, other oxylipins have been found to exert defensive activities by acting as regulators of gene expression (Stintzi et al., 2001; Browse, 2009; Mueller and Berger, 2009) and cell death (De León et al., 2002; Hamberg et al., 2003; Montillet et al., 2005) and as sources of antimicrobial compounds (Prost et al., 2005). Recently, the importance of the 9-LOX pathway in the response of plants to pathogens and pests attack has been unraveled (Hwang and Hwang, 2010; López et al., 2011; Nalam et al., 2012). Genetic studies in Arabidopsis (*Arabidopsis thaliana*) revealed the role of 9-LOX oxylipins in activating local defense against virulent *Pseudomonas syringae* (Hwang and Hwang, 2010; López et al., 2011; Vicente et al., 2012) as well as the cooperation of the 9-LOX and α-dioxygenase pathways in triggering systemic resistance (Vicente et al., 2012). Moreover, strong 9-LOX activity has been found in roots of Arabidopsis plants where 9-LOX products modulate root architecture (Vellosillo et al., 2007).

Studies of the signaling processes mediating the action of 9-LOX derivatives have indicated that their defense activities are in part exerted by modulating hormonal homeostasis (López et al., 2011; Vicente et al., 2012) as well as by inducing defense responses through a JA-independent signaling pathway that might be functionally involved in cell wall modifications (Vellosillo et al., 2007). To further investigate 9-LOX signaling, here we made use of *nonresponding to oxylipins* (*noxy*) mutants having an impaired response to the 9-LOX derivative 9-hydroxy-10,12,15-octadecatrienoic acid (9-HOT). We found that *noxy* mutants showing enhanced susceptibility to *P. syringae* pv *tomato* (*Pst*) were partially insensitive to isoxaben, a herbicide inhibiting cellulose synthesis and triggering cell wall repair responses. Furthermore, identification and characterization of *noxy* mutations provided genetic evidence probing the contribution of mitochondria in signaling 9-LOX- and SA-upregulated defense.

RESULTS

The *noxy2* Mutant, Nonresponding to 9-HOT, Shows Partial Insensitivity to Isoxaben

In order to identify signaling components of the 9-HOT-induced defensive response, we made use of *noxy2-1*, a 9-HOT-insensitive mutant that was isolated in a forward genetic screen based on the root waving activity of 9-HOT. This mutant displayed enhanced susceptibility to avirulent and virulent strains of *P. syringae*, reduced activation of 9-HOT responses (root waving, formation of callose deposits, and expression of 9-HOT-responding genes), and altered root development (Vellosillo et al., 2007). Genetic and map-based cloning studies indicated that the *noxy2-1* mutation was monogenic and recessive and was located in *At5g11630* encoding an uncharacterized protein that we named NOXY2. Confirmation of this was provided by the complementation of the *noxy2-1* phenotypic alterations (root development and 9-HOT sensitivity) by transformation with a genomic clone of *At5g11630* (Supplemental Fig. S1). Further data validating the identification of the *noxy2-1* mutation was the observation that a transfer DNA (T-DNA) insertion mutant (SALK_019745) in *At5g11630* (that we designated as *noxy2-2*) showed, like *noxy2-1*, 9-HOT-insensitivity and altered root development and that both phenotypic alterations were restored by expression of a wild-type version of *At5g11630* under the control of the 35S promoter (*noxy2-2;35S:At5g11630*; Supplemental Fig. S1).

Studies on the response of plants to 9-HOT revealed that the defensive activity of this oxylipin was, at least in part, due to modification of the cell wall (Vellosillo et al., 2007). Therefore, we examined whether *noxy2* mutants differed from wild-type plants in their response to isoxaben, a damaging herbicide inhibiting cellulose synthesis and triggering repair processes and up-regulation of defense-related genes (Caño-Delgado et al., 2003; Manfield et al., 2004; Bischoff et al., 2009; Denness et al., 2011). To this end, seeds from *noxy2-1*, *noxy2-2*, isoxaben-containing medium and examined 7 d after germination. Two mutants, resistant (*ixr1-1*) or hypersensitive (*prc1-1*) to isoxaben, respectively, were included in these analyses (Fagard et al., 2000; Scheible et al., 2001). As shown in Figure 1, A and B, isoxaben caused growth arrest, swelling, and ectopic production of lignin in roots of wild-type seedlings. As expected, no such alterations were observed in *ixr1-1* plants, in which mutation of the cellulose synthase *CESA3* renders an active isoform insensitive to isoxaben (Scheible et al., 2001). Importantly, the two *noxy2* mutants showed partial insensitivity to isoxaben. Thus, whereas isoxaben reduced the length of the primary root of wild-type plants by 83%, this effect diminished to 38% and 3% in *noxy2-1* and *noxy2-2*, respectively (Fig. 1C). In addition, microscopy examination revealed that formation of lignin deposits and root swelling in wild-type plants in response to isoxaben was much less pronounced in *noxy2-1* and *noxy2-2* mutants (Fig. 1, A and B). In contrast to the results with *ixr1-1* and *noxy2* mutants, a clear isoxaben hypersensitivity was found in *pcr1-1* plants, in which loss of *CESA6* function caused a cellulose synthase defect and cellulose deficiency (Fagard et al., 2000; Fig. 1, A–C).

NOXY2 Encodes a Mitochondrial Protein of Unknown Function

Analyses of *NOXY2* expression by means of promoter GUS constructs (*NOXY2:GUS*) revealed GUS activity in cotyledons and roots of transgenic seedlings and in floral tissues of mature plants (Fig. 2A). GUS staining was primarily localized in vascular tissues, lateral root primordia, and root meristems. Increased GUS staining was apparent in cotyledons and roots of 9-HOT- or isoxaben-treated seedlings (Fig. 2, A, B, and D). Also, the

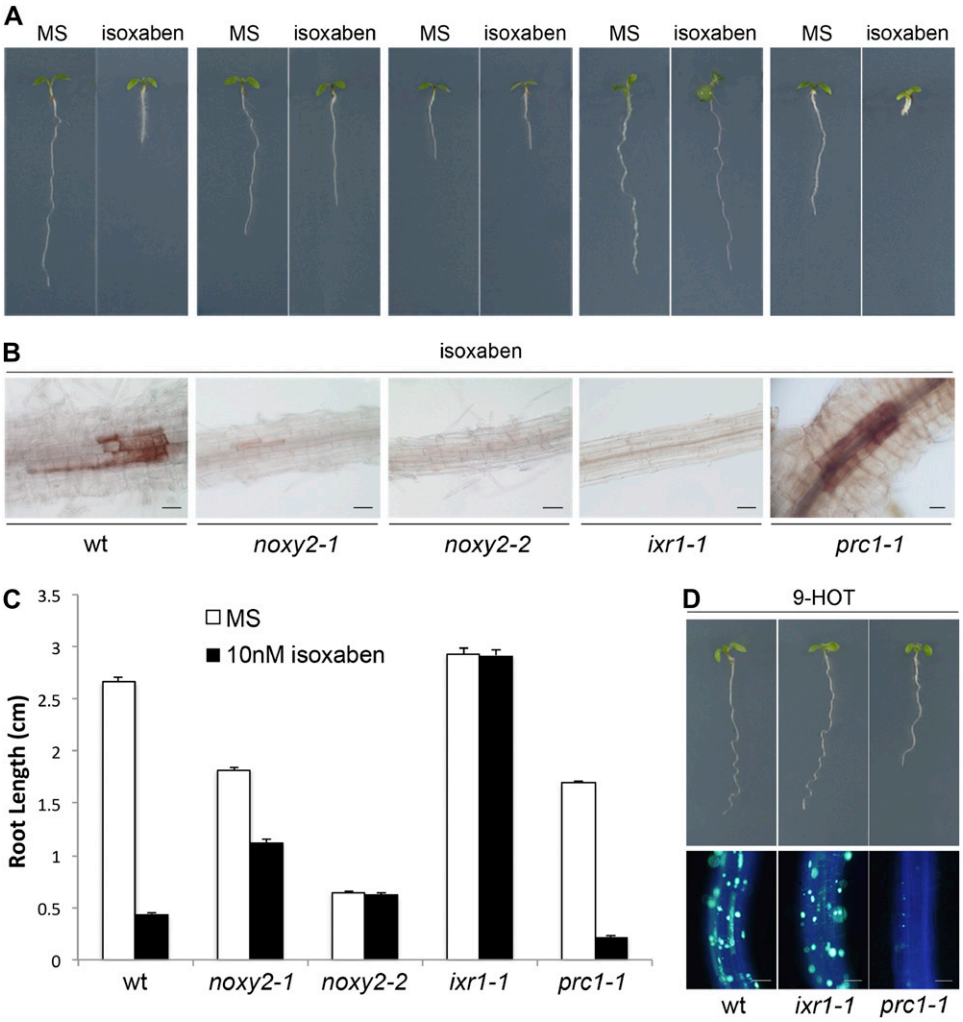

Figure 1. Root phenotypes of wild-type (wt), *noxy2-1*, *noxy2-2*, *ixr1-1*, and *prc1-1* plants responding to isoxaben. A, Transmitted light visualization of seedling grown for 7 d in control MS medium and in isoxaben-containing medium (10 nM). B, Examination of ectopic lignin in roots of isoxaben-treated seedlings stained with phloroglucinol. C, Length of primary roots in 7-d-old seedlings grown in control MS medium and in isoxaben-containing medium (10 nM). The data presented are results obtained in three independent experiments. Means and SE of 60 seedlings are shown. D, Phenotype of seedlings grown for 3 d in MS medium and then transferred to grow for three additional days on 9-HOT-containing medium (25 μM; top panels). Fluorescence visualization of callose deposition in 9-HOT-treated roots stained with aniline blue (bottom panels). Bars = 50 μm.

expression of the *NOXY2*:*GUS* was induced in leaves inoculated with the avirulent bacterial strain *Pst* DC3000 *avrRpm1* or the virulent bacterium *Pst* DC3000, as well as in response to isoxaben infiltration, whereas no induction was observed in water-infiltrated leaves used as a control (Fig. 2, C and D).

Examination of *NOXY2* expression by using semi-quantitative reverse transcription (RT)-PCR revealed the presence of two mRNAs, designated *NOXY2-α* and *NOXY2-β*, that accumulated in response to 9-HOT, bacterial inoculation, and isoxaben (Fig. 2E). Cloning and sequencing of the corresponding complementary DNAs (cDNAs) revealed that these mRNAs are splice variants of *NOXY2* directing the synthesis of proteins (NOXY2-α and NOXY2-β) with 93 and 91 amino acids, respectively. The two proteins were identical in their first 82 amino acids but differed in their C-terminal regions (Fig. 2F). The *NOXY2-α* mRNA reached higher levels than *NOXY2-β* transcripts in the three responses examined, among which isoxaben caused the stronger induction. The phenotypic alterations and the responses to 9-HOT and isoxaben of *noxy2-1* and *noxy2-2* were restored by expression of a wild-type *NOXY2-α* cDNA under the control of the 35S promoter (*35S:NOXY2-α*) but not by expression of *35S:NOXY2-β*, thus indicating a major role of *NOXY2-α* (Supplemental Fig. S2). In these lines, the expression of the two transgenes (*35S:NOXY2-α* and *35S:NOXY2-β*) reached similar levels of accumulation (Supplemental Fig. S2), therefore indicating that the failure of *NOXY2-β* to complement the *noxy2* phenotype was not due to low levels of expression but that NOXY2-α is the functional NOXY2 protein.

Genome analyses indicated that Arabidopsis contains 11 NOXY2 homologs sharing 50% to 60% sequence identity with NOXY2. Nine of the *NOXY2* homologs identified generate distinct mRNA variants encoding proteins that vary in their last amino acids but that are otherwise identical to each other (Supplemental Fig. S3). Apart from *At2g20585* playing an unknown function in polar nuclei fusion during female gametophyte development (Portereiko et al., 2006), no other functions have been assigned to any NOXY2 homolog. Protein alignment revealed a highly conserved 20-amino acid region that contains the *noxy2-1* mutation (a C-to-T transition at nucleotide 188 that converts Ala-63 to Val) and might thus be relevant for protein functionality (Supplemental Fig. S3).

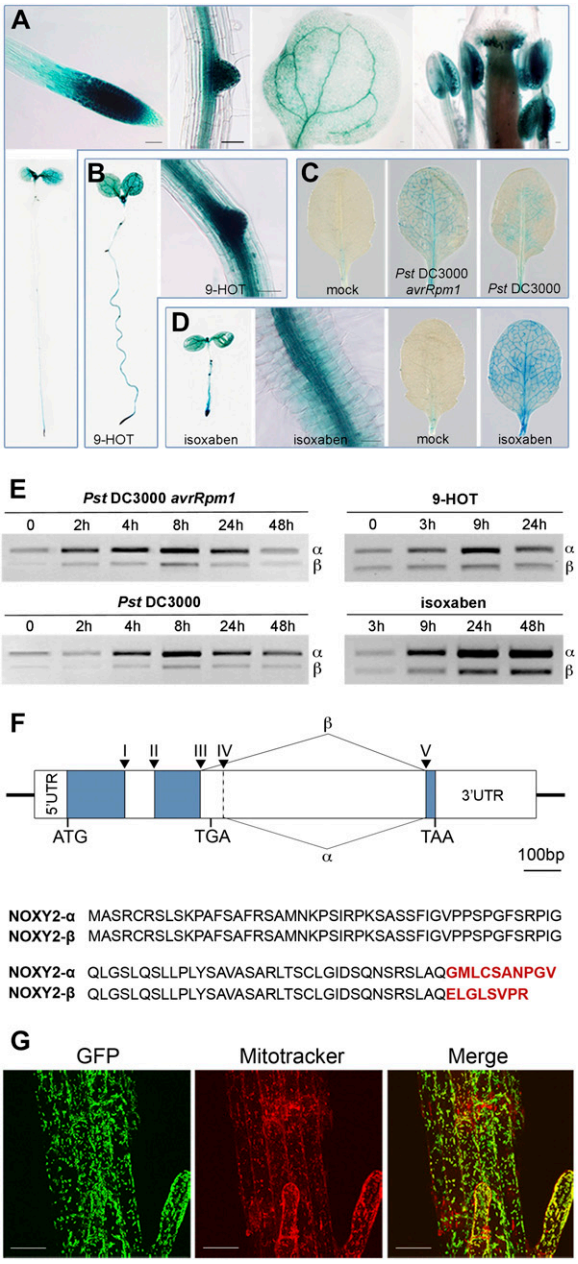

Figure 2. Analysis of *NOXY2* gene expression and localization of NOXY2 protein. A, GUS activity in seedlings, roots, cotyledons, and flowers of transgenic lines containing a *NOXY2* promoter GUS construct (*NOXY2*:*GUS*). B, GUS staining of transgenic seedlings grown in presence of 9-HOT (25 μM). C, Visualization of GUS activity in mature leaves of *NOXY2*:*GUS* plants inoculated with water (mock), *Pst* DC3000 *avrRpm1*, and *Pst* DC3000 (10^8 cfu/mL). D, GUS staining in seedlings of transgenic plants grown in presence isoxaben (10 nM; left panels) and leaves infiltrated with water (mock) or isoxaben (100 nM; right panels). Bars = 50 μm. E, RT-PCR analysis of *NOXY2* transcripts in leaves of wild-type plants responding to *Pst* DC3000 *avrRpm1* and *Pst* DC3000 (10^8 cfu/mL) inoculation and in roots of seedlings responding to 9-HOT (25 μM) and isoxaben (100 nM). Two DNA fragments corresponding to distinct spliced variants of *NOXY2* were identified and designated as α and β, respectively. F, Representation of the *NOXY2* gene with exons shown as blue boxes. Arrowheads indicated splicing sites (numbered from I to V), and lines above and below the *NOXY2* gene show the splicing events generating transcripts β and α, respectively. Alignment of *NOXY2*-α and *NOXY2*-β encoded proteins. C-terminal regions differing between NOXY2-α and NOXY2-β are shown in red. UTR, Untranslated region. G, Subcellular localization of NOXY2 in transgenic *noxy2-1* mutants expressing a NOXY2α-GFP fusion (green). Roots from 7-d-old seedlings expressing the indicated fusion protein were staining with MitoTracker Red CMXRos staining (red). The GFP and MitoTracker images were merged to show the colocalization of the GFP signal at the mitochondria. Bars = 25 μm.

Sequence analyses of NOXY2 indicated the presence of a signal peptide that might target mitochondrial localization. Therefore, we examined the subcellular location of NOXY2 by generating translational fusions in which the GFP protein was fused in frame to the C terminus of the *NOXY2*α cDNA. We used the 35S promoter to express the NOXY2α-GFP fusion (*35S:NOXY2*α*-GFP*) in wild-type controls and *noxy2-1* mutants. The phenotype of *noxy2-1* mutants was partially rescued by expression of the *35S:NOXY2*α*-GFP* (Supplemental Fig. S4), and GFP fluorescence was primarily localized to small but distinct regions (Fig. 2G). Parallel staining with MitoTracker red, a dye that specifically accumulates in the mitochondria, revealed that GFP fluorescence (in *35S:NOXY2*α*-GFP* transgenic plants) colocalized with the fluorescence of MitoTracker red, indicating that NOXY2 is targeted to the mitochondria (Fig. 2G).

9-HOT Shares Signaling Events with Those Triggering Cell Wall Repair Responses

Given that *noxy2* was isolated together with additional *noxy* mutants in a screen for 9-HOT-insensitive plants (Vellosillo et al., 2007), we predicted that additional *noxy* mutations should yield partial insensitivity to isoxaben. Therefore, we examined the phenotype of 40 *noxy* mutants grown in isoxaben-containing medium. In these analyses, we found that 44% of *noxy* mutants respond like *noxy2* plants with smaller reduction of root length, reduced swelling, and reduced formation of lignin deposition compared with wild-type plants (see *noxy15* and *noxy38* as representative examples in Fig. 3A), whereas 29% of *noxy* plants responded like wild-type plants to isoxaben (see *noxy10* and *noxy18* in Fig. 3C). In addition, an intermediate response to isoxaben was found in 27% of *noxy* mutants that were deficient in lignin deposition and root swelling but otherwise showed a similar reduction in root length as seen in wild-type plants (see *noxy21* and *noxy33* as representative examples in Fig. 3B). The fact that 71% of *noxy* mutants were partially insensitive to isoxaben indicates that the *noxy* mutations might impair the ability of plants to activate cell wall repair responses and that the responses to 9-HOT share signaling events with those involved in maintaining the integrity of the cell wall. The finding that the cellulose-deficient *prc1-1* mutant, like the *noxy* plants, was partially insensitive to 9-HOT supported the interplay between the two pathways. (Fig. 1D).

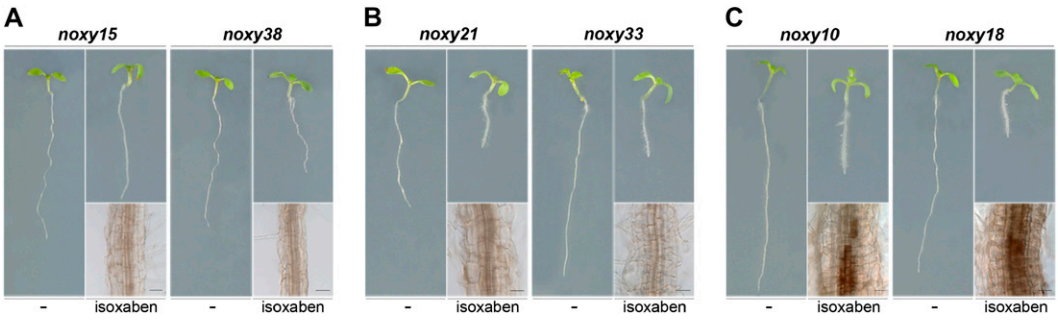

Figure 3. Phenotypes of *noxy* mutants responding to isoxaben. A, Transmitted light visualization of *noxy15* and *noxy38* seedlings grown for 7 d in control MS medium and in isoxaben-containing medium (10 nM). B, Phenotype of *noxy21* and *noxy33* seedlings grown as in A. C, Phenotype of *noxy10* and *noxy18* seedlings grown as in A. Histological examination of ectopic lignin accumulation in isoxaben-treated roots stained with phloroglucinol is shown. Bars = 50 μm.

NOXY2, *NOXY15*, and *NOXY38* Contribute to Plant Defense against Virulent Bacterial Pathogens

Among the 9-HOT-insensitive mutants characterized above, *noxy15* and *noxy38* respond like *noxy2* to isoxaben and were selected for further examination. Since *noxy2-1* showed enhanced susceptibility to *P. syringae* infection (Vellosillo et al., 2007), it seemed likely that also the *noxy15* and *noxy38* mutations should diminish the defense potential of plants. Therefore, we examined the phenotype of *noxy15* and *noxy38* for enhanced susceptibility to *Pst* DC3000. The *noxy2-2* mutant was also included in these studies. No major alterations of the plant phenotype (Supplemental Fig. S5), except for slower shoot growth compared with the wild type, was observed in *noxy* mutants. Three days after bacterial inoculation, growth of *Pst* DC3000 in leaves of *noxy2-2*, *noxy15*, and *noxy38* mutants was higher by factors of 5, 10, and 6, respectively, compared with wild-type controls (Fig. 4A). Accordingly, *noxy2-2*, *noxy15*, and *noxy38* showed stronger disease symptoms than those seen in wild-type plants (Fig. 4B).

A major signal controlling the activation of plant defense against *Pst* DC3000 infection is SA. Therefore, to further characterize the *noxy* mutations, we examined SA-dependent gene expression after SA application. In line with the enhanced susceptibility of *noxy* mutants, transcript abundance of the two SA markers examined *PATHOGENESIS-RELATED1* (*PR1*) and *PR5* was lower in *noxy* mutants than in wild-type plants (Fig. 4, C and D). The diminished capacity of *noxy* mutants to activate SA-mediated up-regulation of gene expression might at least partly explain the reduced defensive potential seen in *noxy* mutants. Moreover, the results indicated that the NOXY2, NOXY15, and NOXY38 proteins play a positive role in plant defense where their activity would contribute to the activation of SA-dependent defense gene expression.

The *noxy2*, *noxy15*, and *noxy38* Mutations Disturb Mitochondrial Morphology and Distribution

Map-based cloning studies indicated that the *noxy15* mutation was located in *At4g33650*, encoding the dynamin-related protein DRP3A known to localize to the outer surface of mitochondria and to play a key role in mitochondrial fission (Fujimoto et al., 2009). The *noxy15* mutation was a G-to-A transition at nucleotide 281 that converts Arg-94 to His at the putative GTPase domain of the DRP3A protein and was renamed *drp3a-1* (Supplemental Fig. S6). Confirmation that *noxy15* impairs mitochondrial fission was obtained by transformation with a mitochondrial-yellow fluorescent protein (YFP) marker (mt-*CD3-990*; Nelson et al., 2007), allowing mitochondrial visualization. Thus, whereas small and discrete mitochondria were visible in transgenic wild-type plants (*Col-0;35S:Mt-YFP*; Fig. 5A), mitochondria in transformed *noxy15* plants (*noxy15;35S:Mt-YFP*) appear connected to each other forming a network of massively elongated mitochondria and large nodule-like structures that likely correspond to mitochondrial aggregates (Fig. 5B).

The *noxy38* mutation was mapped at the *FRIENDLY MITOCHONDRIA* (*FMT*) locus (*At3g52140*), a homolog of the *CluA* gene of *Dictyostelium discoideum* encoding a predicted tetratricopeptide repeat protein playing a role in the correct distribution of mitochondria in the cell (Logan et al., 2003). The *noxy38* mutation is a G-to-A transition in the last nucleotide of intron 22 and was renamed *fmt-1* (Supplemental Fig. S6). Transcripts derived from *fmt-1* include intron 22 and are translated into a predicted truncated protein of 1053 amino acids lacking the tetratricopeptide repeat domain, thought to function in protein-protein interactions. The subcellular localization of FMT is presently unknown; however, in line with previous reports (Logan et al., 2003), Mito-Tracker staining of wild-type and *noxy38* roots reveals the formation of strong mitochondrial aggregates in *noxy38* plants (Fig. 5, C and D).

Because mitochondrial morphology and distribution was altered in *noxy15* and *noxy38* mutants, we examined these organelles in *noxy2* mutants after transformation with the mitochondrial-YFP marker (mt-*CD3-990*; Nelson et al., 2007). Although most mitochondria showed a wild-type distribution and size, nodule-like structures were visible in *noxy2-1* (*noxy2-1;35S:Mt-YFP*) and *noxy2-2* transgenic plants (*noxy2-2;35S:Mt-YFP*; Fig. 5, E and F).

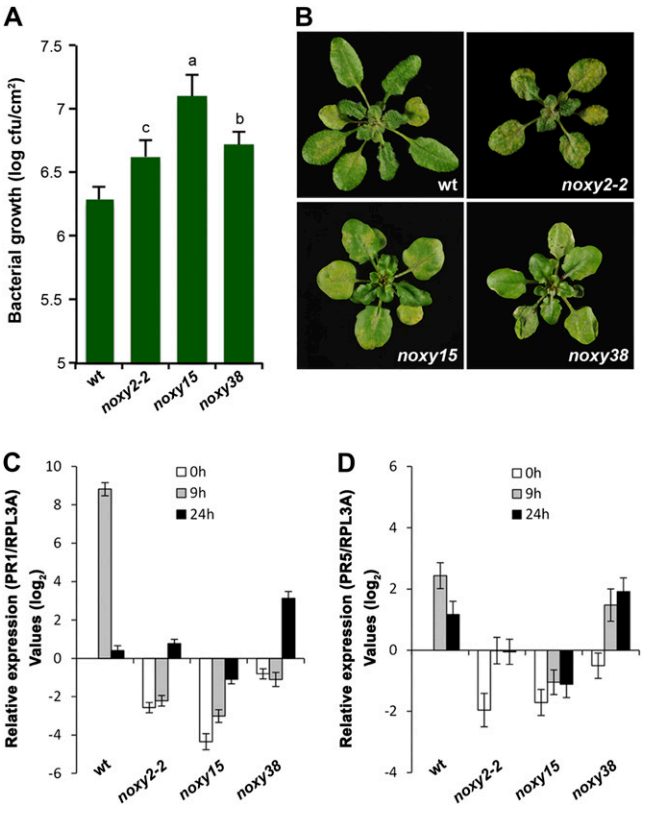

Figure 4. Response of wild-type (wt), *noxy2-2*, *noxy15*, and *noxy38* plants to bacterial infection. A, Bacterial growth in wild-type, *noxy2-2*, *noxy15*, and *noxy38* plants at 72 h after spray inoculation of a suspension of *Pst* DC3000 (10^8 cfu/mL). Means and SE obtained in three independents experiments are shown. Letters on top of the bars indicate statistically significant differences between wild-type and *noxy* plants (Student's *t* test; $P < 0.001$ [a], $0.001 < P < 0.01$ [b], and $0.01 < P < 0.05$ [c]). B, Lesion developed in wild-type, *noxy2-2*, *noxy15*, and *noxy38* plants. Shown are representative examples of symptoms developed at 72 h after spray inoculation. C, Expression of *PR1* was determined by quantitative RT-PCR in RNA samples extracted at intervals times from SA-treated (250 μM) seedlings. Gene *At1g43170* encoding RPL3A was used to normalize transcript levels in each sample. Results shown are the mean of three independent experiments. D, Expression of *PR5* was determined as described in C.

The *noxy2*, *noxy15*, and *noxy38* Mutations Alter Mitochondrial Functionality

Given that plants integrate mitochondrial signals to regulate nuclear gene expression, referred to as retrograde signaling (Rhoads et al., 2006), we predicted that the mitochondrial alterations in *noxy* mutants could negatively impact mitochondrial-nuclei communication. To examine this possibility, we analyzed the expression of mitochondrial alternative oxidase1 (*AOX1a*; *At3g22370*) shown to be under retrograde regulation in response to specific mitochondrial damaging agents, such as antimycin A (Rhoads et al., 2006). Additionally, the expression of a mitochondrial manganese superoxide dismutase (*MSD1*; *At3g10920*) controlling ROS production (Morgan et al., 2008) was similarly examined. Analyses of *AOX1a* and *MSD1* transcript abundance after antimycin A revealed significant differences between wild-type plants and *noxy* mutants (Fig. 5, G and H). The level of *AOX1a* transcripts reached higher levels in *noxy15* and *noxy38* mutants than in wild-type plants, whereas the opposite was observed in *noxy2-2*. In the case of *MSD1*, we observed a weak induction above basal levels in wild-type plants, whereas the level of transcripts in the *noxy* plants examined decreased compared with wild-type plants.

The results of these analyses indicated that the three *noxy* mutations characterized caused an alteration in the response of plants to mitochondrial damage and, thus, that the *noxy* mutations might disturb mitochondrial functionality.

Effect of 9-HOT on Mitochondria

Given that *noxy* mutants disturb mitochondrial morphology and function, we examined whether the application of 9-HOT might exert any effect on mitochondria. As seen in Figure 6A, treatment of seedlings with 9-HOT provoked mitochondrial swelling and aggregation as well as the formation of mitochondrial structures of annular appearance. Clusters of round-shaped mitochondria were preferentially seen in the differentiation zone of the roots, whereas annular structures were mainly found in hypocotyls. Because mitochondrial swelling is frequently associated with a loss of membrane potential (Borutaite, 2010; Schwarzländer et al., 2012b), we also tested whether the application of 9-HOT decreases the membrane potential of mitochondria. In order to assess this possibility, Columbia-0 (Col-0) plants expressing the mitochondrial-YFP fluorescence marker (Nelson et al., 2007) were stained with tetramethyl rhodamine methyl ester (TMRM), a dynamic reporter of mitochondrial membrane potential whose fluorescence is spectrally separated from that of mitochondrial-YFP. As expected, a red signal colocalizing with the mitochondrial-YFP protein was seen after TMRM staining (Fig. 6B). The red and green fluorescence intensities from individual mitochondria were similar in control untreated samples; however, an overall decrease of the TMRM fluorescence (approximately 33%) was seen after the application of 9-HOT (Fig. 6C). The reduction of red fluorescence indicated that 9-HOT caused loss of mitochondrial membrane potential and membrane depolarization.

DISCUSSION

Previously, we showed that the 9-LOX oxylipin pathway participates in the defense of Arabidopsis against hemibiotrophic bacteria and found evidence that the 9-LOX derivative 9-HOT induces cell wall modifications restricting pathogen invasion. Here, we made use of 9-HOT-insensitive mutants (*noxy*) to further examine the molecular events involved in 9-LOX signaling. The *noxy2* mutant showing enhanced susceptibility to avirulent and virulent strains of *P. syringae* was first selected for this study.

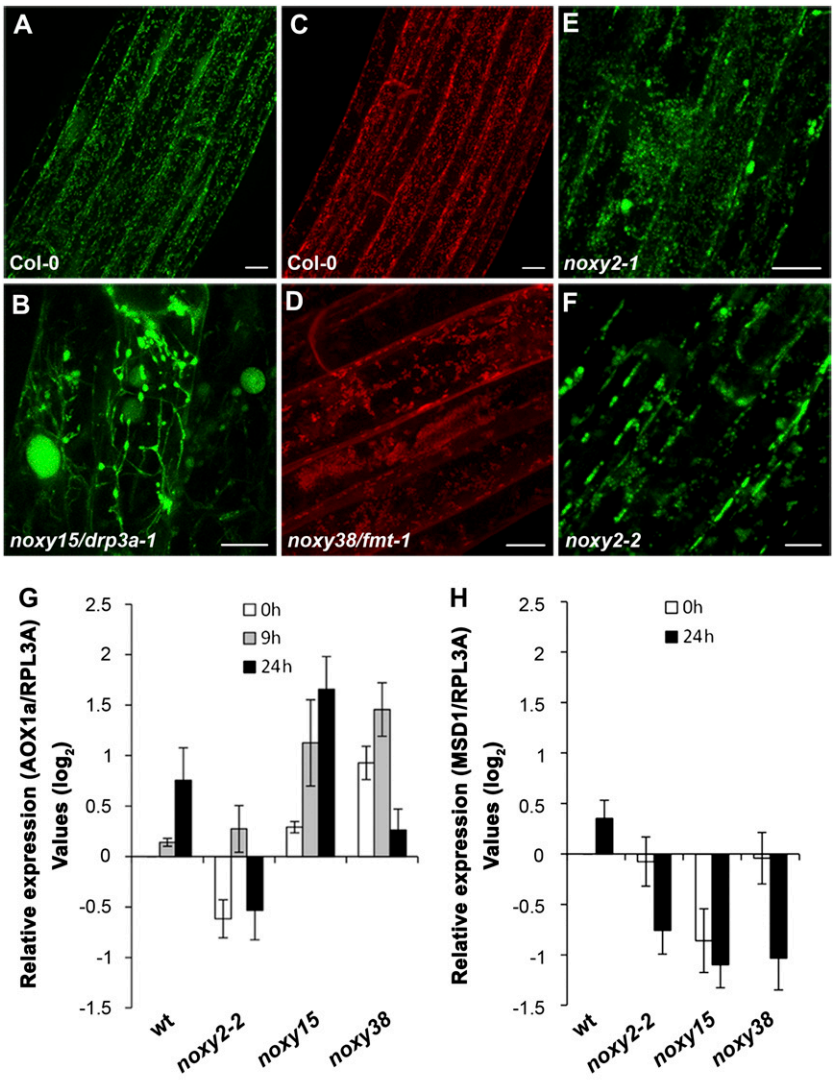

Figure 5. Mitochondrial visualization in roots of Col-0, *noxy2-2*, *noxy15*, and *noxy38* plants. A, Images of mitochondria (green) in transgenic roots of Col-0 expressing a *35S:Mt-YFP* construct. B, Images of mitochondria (green) in transgenic roots of *noxy15/drp3a-1* plants expressing a *35S:Mt-YFP* construct. C, Mitochondrial (red) visualization in roots of Col-0 stained with MitoTracker Red CMXRos. D, Mitochondrial (red) visualization in roots of *noxy38/fmt-1* plants stained with MitoTracker Red CMXRos. E, Images of mitochondria (green) in roots of *noxy2-1* mutant expressing a *35S:Mt-YFP* construct. F, Images of mitochondria (green) in roots of *noxy2-2* mutant expressing a *35S:Mt-YFP* construct. Bars = 10 μm. G, Expression of *AOX1a* was determined by quantitative RT-PCR in RNA samples extracted at different intervals from antimycin A-treated seedlings (20 μM). wt, Wild type. Gene *At1g43170* encoding RPL3A was used to normalize transcript levels in each sample. Results shown are the mean of three independent experiments. H, Expression of *MSD1* was determined as described in G.

In accordance with the role of 9-LOX in plant defense (Hwang and Hwang, 2010; López et al., 2011; Vicente et al., 2012), we found that the expression of *NOXY2* was induced by 9-HOT and bacterial infection. Moreover, consistent with the induction of cell wall changes by 9-HOT, we found that expression of *NOXY2* was induced by isoxaben, an herbicide inhibiting cellulose biosynthesis and triggering cell wall repair and defense responses (Caño-Delgado et al., 2003; Manfield et al., 2004; Bischoff et al., 2009; Denness et al., 2011). The finding that the 9-HOT-insensitive *noxy2* was also partially insensitive to isoxaben indicated that the response of plants to these two compounds share common signaling processes, a conclusion that was strongly supported by the results showing that out of the 41 *noxy* mutants tested (isolated together with *noxy2* in a screen for 9-HOT-insensitive plants), 71% showed partial insensitivity to isoxaben. These results are consistent with a failure of *noxy* mutants in signaling cell wall repair responses and suggested the participation of a high proportion of NOXY proteins in this regulatory pathway. Moreover, the fact that the cellulose-deficient *pcr1-1* mutant was insensitive to 9-HOT (Fig. 1D) suggested that *noxy* mutants might be also altered in the composition of the cell wall. Further examination will be required to ascertain this possibility.

Control of cell wall integrity in plants is needed to allow growth and cell expansion under physiological conditions (Wolf et al., 2012). Moreover, repair and cell wall strengthening mechanisms are critical defense responses to limit pathogen infection (Boller and Felix, 2009; Brutus et al., 2010; Yamaguchi et al., 2010; Denness et al., 2011). In this context, the fact that the 9-HOT-insensitive *noxy2-2*, *noxy15*, and *noxy38* mutants displayed enhanced susceptibility to *P. syringae* infection suggested the participation of NOXY proteins in the signaling processes mediating cell wall-mediated defense. In addition, these results support previous findings pointing to the involvement of 9-HOT and of

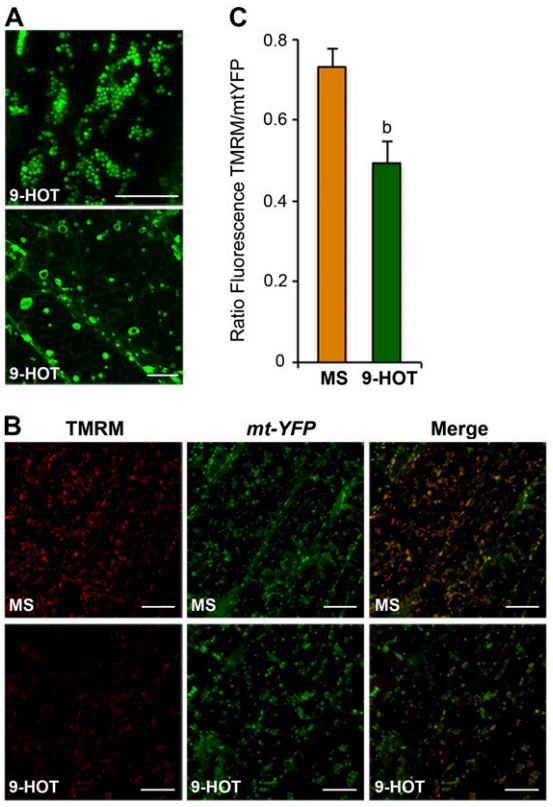

Figure 6. Mitochondrial aggregation and decrease of membrane potential in response to 9-HOT. A, Mitochondrial visualization of 9-HOT-treated (25 μM) transgenic lines expressing *35S:Mt-YFP* revealed the formation of aggregates (top panels) and annular structures (bottom panel). B, TMRM mitochondrial staining (red) and green fluorescence of seedlings expressing *35S:Mt-YFP* (green). Merge of red and green coloration revealed similar fluorescence intensities in individual mitochondria of untreated samples (top panels) and a reduction of TMRM fluorescence after the application of 9-HOT (25 μM; bottom panels). Bars = 10 μm. C, Representation of the TMRM and *mt-YFP* fluorescence intensities measured in untreated and 9-HOT-treated roots. Means and SE of measurements of 15 images are shown. Letters on top of the bars indicate statistically significant differences between control and 9-HOT treatment (Student's *t* test; $0.001 < P < 0.01$ [b]).

the 9-LOX oxylipin pathway in activating cell wall defense responses (Vellosillo et al., 2007). Previous studies with *noxy* mutants demonstrated that enhanced bacterial susceptibility and 9-HOT insensitivity can be the consequence of a constitutive production of ET (López et al., 2011). However, we note that the phenotype of *noxy2-2*, *noxy15*, and *noxy38* does not show the alterations associated with the activation of the ET pathway (short hairy roots); thus, it is unlikely that the defects produced by these mutations could be due to the overproduction of ET.

The identification of NOXY2 as a functionally unknown mitochondrial protein and of *noxy15* (*drpa3-1*) and *noxy38* (*fmt-1*) as new alleles of *DRP3A* encoding a mitochondrial dynamin-related protein (DRPA3; Fujimoto et al., 2009) and *FMT* serving for the distribution of mitochondria in the cell (Logan et al., 2003), respectively, indicated the participation of mitochondria in signaling the response to 9-HOT and in plant defense. Of interest, information found in databases and our own experiments indicated that the three genes identified (*NOXY2*, *NOXY15/DRP3A*, and *NOXY38/FMT*) generate distinct mRNA transcripts and, thus, that the regulation of their expression is subjected to alternative splicing, a widespread mechanism to regulate both protein function and gene expression in plants (Filichkin et al., 2010). Detailed studies on *NOXY2* gene expression revealed that the two spliced variants identified were induced in response to 9-HOT, bacterial inoculation, and isoxaben and that the relative accumulation of the two transcripts examined did not vary during the treatments analyzed (Fig. 2). Besides, we found that only one of the two predicted *NOXY2* encoded proteins, namely, NOXY2-α, complemented the phenotypic alterations found in *noxy2* mutants and, thus, that this protein variant corresponded to the active NOXY2 protein.

Visualization of mitochondria in *noxy* mutants revealed clear alterations in the shape and distribution of these organelles as compared with wild-type plants. This was also the case after examining the response of plants to specific mitochondrial damaging agents such as antimycin A, which can result in the production of mitochondrial ROS (Chang et al., 2012). Because alternative oxidase functions to alleviate mitochondrial stress (Rhoads et al., 2006), the enhanced induction of *AOX1a* expression in *noxy15* and *noxy38* mutants is consistent with an enhanced production of stress signals. By contrast, the reduction of *AOX1a* expression in *noxy2-2* could result from a failure in sensing or responding to mitochondrial damage. Regardless of the detailed mechanisms involved, it may be concluded that the alteration of gene expression observed in the *noxy* mutants examined is likely reflecting a functional perturbation of the mitochondria. Further support for this conclusion came from the results showing reduced expression in *noxy* mutants of *MSD1* encoding a mitochondrial manganese superoxide dismutase that controls ROS production (Morgan et al., 2008).

Additional evidence supporting the participation of mitochondria in 9-HOT signaling was the observation that 9-HOT provoked the formation of mitochondrial aggregates and annular mitochondrial structures as well as a loss of membrane potential and, as a consequence, the depolarization of the mitochondrial membrane. Mitochondrial changes similar to those induced by 9-HOT were produced after generation of superoxide ion in Arabidopsis plants (Scott and Logan, 2008). Moreover, mitochondrial swelling and aggregation was found to accompany the response to elevated temperatures in yeast (Kawai et al., 2001) and to precede apoptosis and innate immune responses in vertebrates where aggregation of these organelles might help to increase the concentration of signals (Haga et al., 2003; Arnoult et al., 2011). Similarly, the loss of membrane potential has been shown to be

associated with mitochondrial swelling, which in turn might serve to facilitate solute exchange and the communication between the mitochondria and the cytosol (Borutaite, 2010; Schwarzländer et al., 2012b).

Numerous studies have proven the direct link between mitochondria and innate immunity signaling in vertebrates, in which these organelles play a crucial role in regulating host immunity (Arnoult et al., 2011). Also, a role of these organelles in plant defense responses is emerging from recent results showing that, as found in *noxy* mutants, suppression of innate immunity and reduced SA up-regulation of gene expression may be linked to mitochondrial dysfunction (Block et al., 2010; Gleason et al., 2011) and that up-regulation of defense gene expression might be under mitochondrial retrograde control (Schwarzländer et al., 2012a). The results point to the participation of mitochondria during the activation of plant immunity resulting in a robust resistance response to protect plant tissues against pathogen infection.

MATERIALS AND METHODS

Plants and Growth Conditions

Arabidopsis (*Arabidopsis thaliana*) wild-type plants and *ixr1-1* and *prc1-1* mutants used in this study were derived from Arabidopsis plants ecotype Col-0. For in vitro analyses, sterilized seeds were vernalized for 3 d at 4°C and allowed to grow on media plates. Growth conditions were 14 h of light, 10 h of dark, 22°C and 250 μE m^{-2} s^{-1} fluorescent illumination. For phenotypic examination after 9-HOT and isoxaben treatments, seeds were germinated in vertical plates and transferred 4 d after germination to plates containing the products of interest (9-HOT, 25 μM; isoxaben, 10 nM). For examining gene expression, seeds were germinated in horizontal plates and treated 12 d after germination with SA (250 μM) and antimycin A (20 μM). For in planta analyses, seeds were sown on soil, vernalized for 3 d at 4°C, and grown in a chamber at 22° and 70% relative humidity under a 14-h-light, 10-h-dark photoperiod at 250 μE m^{-2} s^{-1} fluorescent illumination. Plants were treated and examined between 3 and 4 weeks after seed germination.

In Vivo Analyses of Bacterial Growth

Bacterial inoculations were performed under greenhouse conditions by spraying a suspension (10^8 colony-forming units [cfu]/mL) onto the leaf surface. The bacterial strains used in this study were *Pst* DC3000 *avrRpm1* (avirulent) and *Pst* DC3000 (virulent). Prior to spray inoculation, bacteria were grown overnight at 28°C in petri plates with King's B medium. Bacterial suspensions were prepared in 10 mM $MgCl_2$ containing 0.04% (v/v) Silwet L77. Discs from infected leaves were excised at the times of interest, pooled in triplicate, homogenized, and used for counting bacterial growth in petri plates. Reported results are the means and SE of the values obtained in three independent experiments.

Preparation of 9-HOT

9-HOT was prepared by stirring linolenic acid (120 mg) at 23°C with tomato (*Solanum lycopersicum*) whole homogenate under an atmosphere of oxygen essentially as described by Matthew et al. (1977). The product was subjected to open-column silicic acid chromatography to provide more than 95% pure 9(*S*)-HPOT (70 mg). Treatment with sodium borohydride (100 mg) in methanol (10 mL) at 0°C for 30 min followed by preparative straight-phase HPLC using 2-propanol/hexane/acetic acid (2.2:97.8:0.005, v/v/v) as the mobile phase afforded more than 99% pure 9-HOT as a colorless oil (44 mg; yield, 35% from starting linolenic acid). 9-HOT stock was prepared in 95% ethanol and diluted with water to reach the concentration used in these studies.

RNA Isolation and Analyses of Gene Expression

For extraction of RNA, plant tissues were collected at different time intervals, frozen in liquid nitrogen, and stored at −80°C until analysis. Total RNA was isolated according to Logemann et al. (1987). RT-PCR was performed with a GeneAmp PCR System 9700 thermal cycler (Applied Biosystems) using the Titan One Tube RT-PCR system (Roche Applied Science) as specified by the manufacturer. Total RNA was treated with DNase TURBO DNA-free (Ambion) to remove contaminating DNA. One hundred nanograms of this RNA were used in each one-step RT-PCR reaction. Amplification and sequencing of *NOXY2* cDNAs was performed with 5′ and 3′ RACE (Invitrogen). Quantification of gene expression was performed by quantitative RT-PCR analyses using a GeneAmp PCR system 9700 thermal cycler (Applied Biosystems) and the FastStart Universal SYBR Green Master (Rox) system as specified by the manufacturer (Roche). Gene *At1g43170* encoding RPL3A was used as an internal control. Primers used for these analyses and lengths of amplification products are described in Supplemental Table S1.

Construction of Chimeric Constructs and Generation of Transgenic Lines

Genomic and cDNA *NOXY2* sequences were used to prepare chimera constructs using standard procedures. DNA fragments were PCR amplified using Expand High Fidelity polymerase (Roche). Forward and reversed primers used in each case are shown in Supplemental Table S1. DNA-amplified PCR fragments were inserted into appropriated Gateway plasmids and mobilized to *Agrobacterium tumefaciens* for plant transformation.

Mapping and Cloning of *noxy2-1*, *noxy15*, and *noxy38* Genes

For mapping purposes, *noxy2-1*, *noxy15*, and *noxy38* plants (derived from the Col-0 accession) were crossed to wild-type plants of the Landsberg *erecta* ecotype, and F2 mutants were selected. DNA from *noxy2-1* and *noxy15* recombinants was prepared and used to analyze linkage of the mutations to simple sequence length polymorphic and cleaved-amplified polymorphic sequence markers (http://www.arabidopsis.org, http://bar.utoronto.ca). Sequencing of candidate genes was performed to identify the *noxy2-1* and *noxy15* mutations. Mapping of the *noxy38* was performed at the Instituto de Bioengeniería, Universidad Miguel Hernández Gene Mapping Facility (Elche, Spain) as described by Ponce et al. (2006). In brief, for low-resolution mapping, the DNA of 50 F2 phenotypically mutant plants was individually extracted and used as a template to multiplex PCR coamplify 32 simple sequence length polymorphic and insertion/deletion molecular markers using fluorescently labeled oligonucleotides as primers. For fine mapping, 400 additional F2 plants were used to assess linkage between *noxy38* and molecular markers designed according to the polymorphisms between Landsberg *erecta* and Col-0 described at the Monsanto Arabidopsis Polymorphism Collection database (http://www.arabidopsis.org). Massive genome sequencing performed at BIG genomic (http://www.genomics.cn) was used for the identification of the *noxy38* mutation.

Protein Sequence Analysis

NOXY2 homolog proteins were identified in databases using the BLAST program available at the Nation Center for Biotechnology Information GenBank and The Arabidopsis Information Resource. Multiple sequence alignment was performed using ClustalW sequence program. Alignment was graphically displayed using the Jalview alignment editor with ClustalX color scheme (Waterhouse et al., 2009).

Histochemical Analyses

Examination of GUS activity in *NOXY2:GUS* transgenic plants was performed as described by Vellosillo et al. (2007). For the detection of callose, plant tissues were stained and visualized as described by Vellosillo et al. (2007). For the detection of lignin, roots were stained with 2% phloroglucinol-HCl as described by Schrick et al. (2004). For visualization of mitochondria, roots were stained with MitoTracker Red CMXRos (M-7512; Invitrogen) as described by Hedtke et al. (1999). The membrane potential of mitochondria was assessed in hypocotyl cells using the cationic lipophilic fluorescent dye

TMRM. Whole seedlings were equilibrated in 25 nM TMRM (in 0.5× Murashige and Skoog [MS] medium) for 30 min before use. For treatment with 9-HOT, seedlings were incubated in 0.5× MS medium containing 25 μM 9-HOT for 30 min. Fluorescent images of GFP, MitoTracker, and TMRM were generated on a Leica TCS-SP5 confocal microscope with LAS AF version 2.6.0 software, using a 63×/1.2-numerical aperture water immersion objective and sequential scanning with argon 488-nm (GFP) and diode-pumped solid-state 561-nm (MitoTracker and TMRM) laser lines.

Sequence data from this article can be found in the GenBank/EMBL data libraries under accession numbers At5g11630, At4g33650, and At3g52140.

Supplemental Data

The following materials are available in the online version of this article.

Supplemental Figure S1. Complementation of *noxy2-1* and *noxy2-2* by transformation with the wild-type *NOXY2* gene.

Supplemental Figure S2. Complementation of *noxy2-1* and *noxy2-2* by transformation with *NOXY2-α*.

Supplemental Figure S3. Alignment and schematic representation of NOXY2 and of homologous genes present in the Arabidopsis genome.

Supplemental Figure S4. Transformation with *35S:NOXY2-α-GFP* complements the *noxy2-1* phenotype.

Supplemental Figure S5. Phenotypes of *noxy* mutants.

Supplemental Figure S6. Map-based cloning of *noxy15/drp3a-1* and *noxy38/fmt-1*.

Supplemental Table S1. Sets of primers used in this study.

ACKNOWLEDGMENTS

We thank Shauna Somerville and Chris Somerville (Energy Biosciences Institute, University of California, Berkeley) and Roberto Solano and Yovanny Izquierdo (Centro Nacional de Biotecnología, Madrid, Spain) for critical reading of the article and stimulating discussions; Marta Martínez (Centro Nacional de Biotecnología, Madrid, Spain) for help with expression analyses; Juan Carlos Sánchez Ferrero (Centro Nacional de Biotecnología, Madrid, Spain) for protein sequence analyses; R. Piqueras (Centro Nacional de Biotecnología, Madrid, Spain) for help with in vitro plant growth; I. Poveda (Centro Nacional de Biotecnología, Madrid, Spain) for expert photography; and G. Hamberg (Karolinska Institutet, Stockholm, Sweden) for assistance during the preparation of the oxylipins used. We thank Maria Rosa Ponce and Jose Luis Micol (Instituto de Bioengeniería, Universidad Miguel Hernández, Elche, Spain) for their help with the positional cloning of the *NOXY38* gene. The T-DNA insertion line used in this study was from the SALK collection and obtained from the Nottingham Arabidopsis Stock Centre (http://arabidopsis.info).

Received September 17, 2012; accepted December 8, 2012; published December 12, 2012.

LITERATURE CITED

Andreou A, Brodhun F, Feussner I (2009) Biosynthesis of oxylipins in non-mammals. Prog Lipid Res **48:** 148–170

Arnoult D, Soares F, Tattoli I, Girardin SE (2011) Mitochondria in innate immunity. EMBO Rep **12:** 901–910

Bischoff V, Cookson SJ, Wu S, Scheible WR (2009) Thaxtomin A affects CESA-complex density, expression of cell wall genes, cell wall composition, and causes ectopic lignification in *Arabidopsis thaliana* seedlings. J Exp Bot **60:** 955–965

Blée E (2002) Impact of phyto-oxylipins in plant defense. Trends Plant Sci **7:** 315–322

Block A, Guo M, Li G, Elowsky C, Clemente TE, Alfano JR (2010) The *Pseudomonas syringae* type III effector HopG1 targets mitochondria, alters plant development and suppresses plant innate immunity. Cell Microbiol **12:** 318–330

Boller T, Felix G (2009) A renaissance of elicitors: perception of microbe-associated molecular patterns and danger signals by pattern-recognition receptors. Annu Rev Plant Biol **60:** 379–406

Borutaite V (2010) Mitochondria as decision-makers in cell death. Environ Mol Mutagen **51:** 406–416

Browse J (2009) Jasmonate passes muster: a receptor and targets for the defense hormone. Annu Rev Plant Biol **60:** 183–205

Brutus A, Sicilia F, Macone A, Cervone F, De Lorenzo G (2010) A domain swap approach reveals a role of the plant wall-associated kinase 1 (WAK1) as a receptor of oligogalacturonides. Proc Natl Acad Sci USA **107:** 9452–9457

Caño-Delgado A, Penfield S, Smith C, Catley M, Bevan M (2003) Reduced cellulose synthesis invokes lignification and defense responses in *Arabidopsis thaliana*. Plant J **34:** 351–362

Chang R, Jang CJ, Branco-Price C, Nghiem P, Bailey-Serres J (2012) Transient MPK6 activation in response to oxygen deprivation and reoxygenation is mediated by mitochondria and aids seedling survival in Arabidopsis. Plant Mol Biol **78:** 109–122

De León IP, Sanz A, Hamberg M, Castresana C (2002) Involvement of the Arabidopsis alpha-DOX1 fatty acid dioxygenase in protection against oxidative stress and cell death. Plant J **29:** 61–62

Denness L, McKenna JF, Segonzac C, Wormit A, Madhou P, Bennett M, Mansfield J, Zipfel C, Hamann T (2011) Cell wall damage-induced lignin biosynthesis is regulated by a reactive oxygen species- and jasmonic acid-dependent process in Arabidopsis. Plant Physiol **156:** 1364–1374

Dodds PN, Rathjen JP (2010) Plant immunity: towards an integrated view of plant-pathogen interactions. Nat Rev Genet **11:** 539–548

Durand T, Bultel-Poncé V, Guy A, Berger S, Mueller MJ, Galano JM (2009) New bioactive oxylipins formed by non-enzymatic free-radical-catalyzed pathways: the phytoprostanes. Lipids **44:** 875–888

Fagard M, Desnos T, Desprez T, Goubet F, Refregier G, Mouille G, McCann M, Rayon C, Vernhettes S, Höfte H (2000) PROCUSTE1 encodes a cellulose synthase required for normal cell elongation specifically in roots and dark-grown hypocotyls of *Arabidopsis*. Plant Cell **12:** 2409–2424

Filichkin SA, Priest HD, Givan SA, Shen R, Bryant DW, Fox SE, Wong WK, Mockler TC (2010) Genome-wide mapping of alternative splicing in *Arabidopsis thaliana*. Genome Res **20:** 45–58

Fonseca S, Chico JM, Solano R (2009) The jasmonate pathway: the ligand, the receptor and the core signalling module. Curr Opin Plant Biol **12:** 539–547

Fujimoto M, Arimura S, Mano S, Kondo M, Saito C, Ueda T, Nakazono M, Nakano A, Nishimura M, Tsutsumi N (2009) Arabidopsis dynamin-related proteins DRP3A and DRP3B are functionally redundant in mitochondrial fission, but have distinct roles in peroxisomal fission. Plant J **58:** 388–400

Glazebrook J (2005) Contrasting mechanisms of defense against biotrophic and necrotrophic pathogens. Annu Rev Phytopathol **43:** 205–227

Gleason C, Huang S, Thatcher LF, Foley RC, Anderson CR, Carroll AJ, Millar AH, Singh KB (2011) Mitochondrial complex II has a key role in mitochondrial-derived reactive oxygen species influence on plant stress gene regulation and defense. Proc Natl Acad Sci USA **108:** 10768–10773

Haga N, Fujita N, Tsuruo T (2003) Mitochondrial aggregation precedes cytochrome c release from mitochondria during apoptosis. Oncogene **22:** 5579–5585

Hamberg M, Ponce de León I, Sanz A, Castresana C (2002) Fatty acid alpha-dioxygenases. Prostaglandins Other Lipid Mediat **68-69:** 363–374

Hamberg M, Sanz A, Rodriguez MJ, Calvo AP, Castresana C (2003) Activation of the fatty acid alpha-dioxygenase pathway during bacterial infection of tobacco leaves. Formation of oxylipins protecting against cell death. J Biol Chem **278:** 51796–51805

Hedtke B, Meixner M, Gillandt S, Richter E, Börner T, Weihe A (1999) Green fluorescent protein as a marker to investigate targeting of organellar RNA polymerases of higher plants in vivo. Plant J **17:** 557–561

Hwang IS, Hwang BK (2010) The pepper 9-lipoxygenase gene *CaLOX1* functions in defense and cell death responses to microbial pathogens. Plant Physiol **152:** 948–967

Kawai A, Nishikawa S, Hirata A, Endo T (2001) Loss of the mitochondrial Hsp70 functions causes aggregation of mitochondria in yeast cells. J Cell Sci **114:** 3565–3574

Logan DC, Scott I, Tobin AK (2003) The genetic control of plant mitochondrial morphology and dynamics. Plant J **36:** 500–509

Logemann J, Schell J, Willmitzer L (1987) Improved method for the isolation of RNA from plant tissues. Anal Biochem **163:** 16–20

López MA, Bannenberg G, Castresana C (2008) Controlling hormone signaling is a plant and pathogen challenge for growth and survival. Curr Opin Plant Biol **11:** 420–427

López MA, Vicente J, Kulasekaran S, Vellosillo T, Martínez M, Irigoyen ML, Cascón T, Bannenberg G, Hamberg M, Castresana C (2011) Antagonistic role of 9-lipoxygenase-derived oxylipins and ethylene in the control of oxidative stress, lipid peroxidation and plant defence. Plant J **67:** 447–458

Manfield IW, Orfila C, McCartney L, Harholt J, Bernal AJ, Scheller HV, Gilmartin PM, Mikkelsen JD, Paul Knox J, Willats WG (2004) Novel cell wall architecture of isoxaben-habituated Arabidopsis suspension-cultured cells: global transcript profiling and cellular analysis. Plant J **40:** 260–275

Matthew JA, Chan HW, Galliard T (1977) A simple method for the preparation of pure 9-D-hydroperoxide of linoleic acid and methyl linoleate based on the positional specificity of lipoxygenase in tomato fruit. Lipids **12:** 324–326

Montillet JL, Chamnongpol S, Rustérucci C, Dat J, van de Cotte B, Agnel JP, Battesti C, Inzé D, Van Breusegem F, Triantaphylidès C (2005) Fatty acid hydroperoxides and H2O2 in the execution of hypersensitive cell death in tobacco leaves. Plant Physiol **138:** 1516–1526

Morgan MJ, Lehmann M, Schwarzländer M, Baxter CJ, Sienkiewicz-Porzucek A, Williams TC, Schauer N, Fernie AR, Fricker MD, Ratcliffe RG, et al (2008) Decrease in manganese superoxide dismutase leads to reduced root growth and affects tricarboxylic acid cycle flux and mitochondrial redox homeostasis. Plant Physiol **147:** 101–114

Mueller MJ, Berger S (2009) Reactive electrophilic oxylipins: pattern recognition and signalling. Phytochemistry **70:** 1511–1521

Nalam VJ, Keeretaweep J, Sarowar S, Shah J (2012) Root-derived oxylipins promote green peach aphid performance on *Arabidopsis* foliage. Plant Cell **24:** 1643–1653

Nelson BK, Cai X, Nebenführ A (2007) A multicolored set of in vivo organelle markers for co-localization studies in Arabidopsis and other plants. Plant J **51:** 1126–1136

Ponce MR, Robles P, Lozano FM, Brotóns MA, Micol JL (2006) Low-resolution mapping of untagged mutations. Methods Mol Biol **323:** 105–113

Portereiko MF, Sandaklie-Nikolova L, Lloyd A, Dever CA, Otsuga D, Drews GN (2006) NUCLEAR FUSION DEFECTIVE1 encodes the Arabidopsis RPL21M protein and is required for karyogamy during female gametophyte development and fertilization. Plant Physiol **141:** 957–965

Prost I, Dhondt S, Rothe G, Vicente J, Rodriguez MJ, Kift N, Carbonne F, Griffiths G, Esquerré-Tugayé MT, Rosahl S, et al (2005) Evaluation of the antimicrobial activities of plant oxylipins supports their involvement in defense against pathogens. Plant Physiol **139:** 1902–1913

Rhoads DM, Umbach AL, Subbaiah CC, Siedow JN (2006) Mitochondrial reactive oxygen species. Contribution to oxidative stress and interorganellar signaling. Plant Physiol **141:** 357–366

Robert-Seilaniantz A, Grant M, Jones JD (2011) Hormone crosstalk in plant disease and defense: more than just jasmonate-salicylate antagonism. Annu Rev Phytopathol **49:** 317–343

Scheible WR, Eshed R, Richmond T, Delmer D, Somerville C (2001) Modifications of cellulose synthase confer resistance to isoxaben and thiazolidinone herbicides in Arabidopsis Ixr1 mutants. Proc Natl Acad Sci USA **98:** 10079–10084

Schrick K, Fujioka S, Takatsuto S, Stierhof YD, Stransky H, Yoshida S, Jürgens G (2004) A link between sterol biosynthesis, the cell wall, and cellulose in Arabidopsis. Plant J **38:** 227–243

Schwarzländer M, König AC, Sweetlove LJ, Finkemeier I (2012a) The impact of impaired mitochondrial function on retrograde signalling: a meta-analysis of transcriptomic responses. J Exp Bot **63:** 1735–1750

Schwarzländer M, Logan DC, Johnston IG, Jones NS, Meyer AJ, Fricker MD, Sweetlove LJ (2012b) Pulsing of membrane potential in individual mitochondria: a stress-induced mechanism to regulate respiratory bioenergetics in *Arabidopsis*. Plant Cell **24:** 1188–1201

Scott I, Logan DC (2008) Mitochondrial morphology transition is an early indicator of subsequent cell death in Arabidopsis. New Phytol **177:** 90–101

Spoel SH, Loake GJ (2011) Redox-based protein modifications: the missing link in plant immune signalling. Curr Opin Plant Biol **14:** 358–364

Stintzi A, Weber H, Reymond P, Browse J, Farmer EE (2001) Plant defense in the absence of jasmonic acid: the role of cyclopentenones. Proc Natl Acad Sci USA **98:** 12837–12842

Torres MA, Jones JD, Dangl JL (2006) Reactive oxygen species signaling in response to pathogens. Plant Physiol **141:** 373–378

Vellosillo T, Martínez M, López MA, Vicente J, Cascón T, Dolan L, Hamberg M, Castresana C (2007) Oxylipins produced by the 9-lipoxygenase pathway in *Arabidopsis* regulate lateral root development and defense responses through a specific signaling cascade. Plant Cell **19:** 831–846

Vellosillo T, Vicente J, Kulasekaran S, Hamberg M, Castresana C (2010) Emerging complexity in reactive oxygen species production and signaling during the response of plants to pathogens. Plant Physiol **154:** 444–448

Vicente J, Cascón T, Vicedo B, García-Agustín P, Hamberg M, Castresana C (2012) Role of 9-lipoxygenase and α-dioxygenase oxylipin pathways as modulators of local and systemic defense. Mol Plant **5:** 914–928

Waterhouse AM, Procter JB, Martin DMA, Clamp M, Barton GJ (2009) Jalview Version 2: a multiple sequence alignment editor and analysis workbench. Bioinformatics **25:** 1189–1191

Wolf S, Hématy K, Höfte H (2012) Growth control and cell wall signaling in plants. Annu Rev Plant Biol **63:** 381–407

Wu J, Baldwin IT (2010) New insights into plant responses to the attack from insect herbivores. Annu Rev Genet **44:** 1–24

Yamaguchi Y, Huffaker A, Bryan AC, Tax FE, Ryan CA (2010) PEPR2 is a second receptor for the Pep1 and Pep2 peptides and contributes to defense responses in *Arabidopsis*. Plant Cell **22:** 508–522